Thermodynamic evaluation of electrical responses to odorant in olfactory sensory neurons

Samantha Hagerty, Melissa Singletary, Oleg Pustovyy, Ludmila Globa, Edward E. Morrison, Iryna Sorokulova, and Vitaly Vodyanoy*

College of Veterinary Medicine, Auburn University, Auburn AL 36849
*Corresponding author
vodyavi@auburn.edu

Olfactometer

The diagram of the olfactometer is shown in Figure S1. The olfactometer is controlled by the Warner VT-8 software that programmed to generate the experimental sequence of odorant flow and exhausting.

The computer (PC) sends a signal to the the Pneumatic PicoPump PV800 (World Precision Instruments) to open one of six Oxygen Clean 2-way normally closed electronic valves (EV1) installed in the 6-port Oxygen Clean Manifold (Clippard Instrument Laboratory, Manifold 1) (Figure S2). When the electronic manifold valve is open, the corresponding LED control light is on, and air enters from the Air Tank into the Miniature Clippard Air Flow Control Valve (Valve 1), then through the W.A. Hammond Drierite Laboratory Gas Drying Unit (Filter1) the air goes through the open Manifold 1 electronic valve (EV), the first Clippard Unidirectional Valve (VU1), the head space of 100mL bottle (Bottles), the second Clippard Unidirectional Valve (VU2), then following through the corresponding normally open channel of the Clippard Manifold 2 (Figure S2) it streams via the second Miniature Clippard Air Flow Control Valve (Valve 2) to the Clippard Pressure Regulator (PR), DT-8890CEM Ruby-electronics Digital Differential Air Vapor Pressure Meter Gauge Manometer (Manometer), and finally the air with odorant exits the olfactometer and enters OE chamber via a glass nozzle.

At the end of activation time the Pneumatic PicoPump PV800 closes the electronic valve in the Manifold 1 and simultaneously opens the Oxygen Clean 2-way normally closed electronic valve (EV) and the Negative Air Pressure source (VP) in the applicator exhaust path. The air with odorant is cleared the nozzle, Valve 2, the open channel of Manifold 2, valve EV, and W.A. Hammond Carbon Filter (Filter 2). After the end of the exhaust time the valve EV and the the Negative Air Pressure source are shut off and the system rests 20 s before a new activation begins. The olfactometer is synchronized with p-clamp system. Fifty ml glass bottles were used for generation of odorants in the bottle headspaces (Figure S2. Two holes are drilled in the screw-on caps of these bottles to accommodate two Clippard Unidirectional Valves for incoming air and out coming air/odorant/particles.

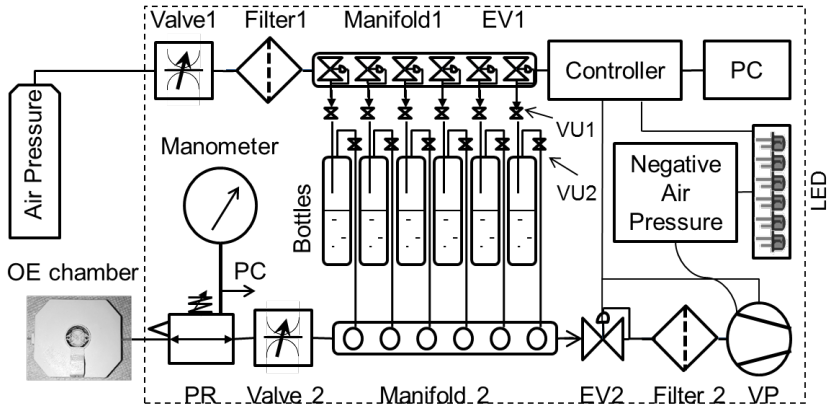

Figure S1. Schematic diagram of olfactometer.

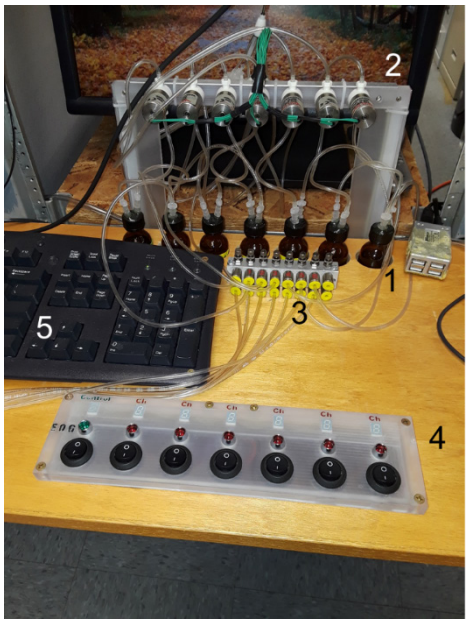

Figure S2. Olfactometer. 1. Glass bottles with odorant solution. The odorant vapor of head space of the bottles is used for activation of EOG. 2. Manifold 1 with electrically controlled valves. 3. Manifold 2 with valves. 4. Manually controlled switches of the valves. 5. Computer keyboard.

EOG measurement system

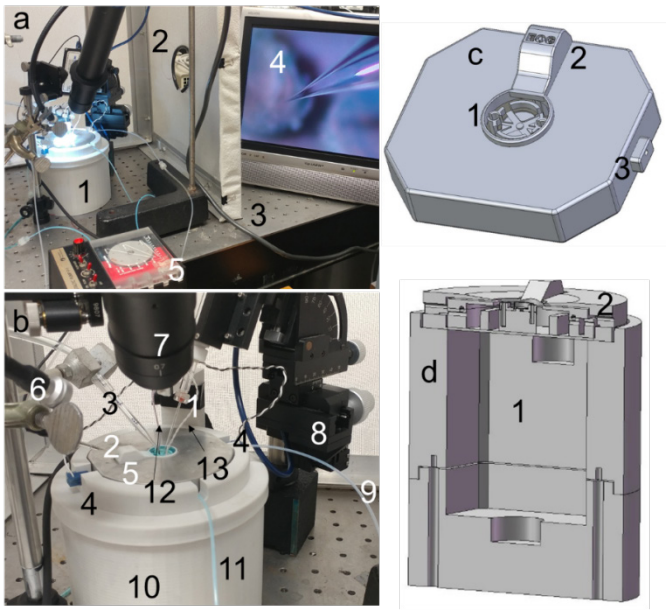

Figure S3. Set up for measurement EOG in isolated olfactory epithelium (OE). a. General overview of the set up. 1-thermostat with perfusion chamber. 2-Graunded Faraday box. 3-vibration isolation table. 4-Video screen. 5-perfusion pump. b. Close up of the thermostat, perfusion chamber, and electrodes. 1-EOG class electrode and holder. 2-Reference electrode port and Ag/AgCl electrode. 3-Glass nozzle for delivery of odorant. 4. Heating leads. 5-perfusion chamber with cover. 6-Light. 7-Video camera. 8-Micromanipulator. 9-Tube with negative air pressure for removing odorant. 10-Thermostat. 11-Incoming perfusion tube. 12 Thermistor. Feedback thermistor. c-Perfusion chamber. 1-Pefused cavity for position of OE. 2-Reference electrode port. d-Cross-section of thermostat. 1-Ice compartment. 2-perfusion chamber.

The EOG measurement arrangement that includes perfusion chamber (b, 5) electrodes (b, 1, 2), thermostat (a,1), and optics (b 6, 7) are covered with a Faraday box (a,2) and positioned onto an antivibration platform (a, 3). The perfusion chamber is filled with a buffer solution by the perfusion pump (a, 5) through the incoming tube (b, 11), and fragment of OE is positioned in the perfusion cavity of the perfusion chamber (c, 1). The class patch clamp electrode (b, 1) is connected to OE and sends electrical signal the patch-clamp (not shown). The reference electrode closes the electric circuit and comes into the reference electrode port (b, 2; c, 2). The tip of the patch-clamp electrode is observed through the video camera (b, 7) and the video-screen (a, 4). The temperature is maintained by the thermostat (a, 1). The temperature of the OE is measured by the thermistor (b, 12) and the feedback thermistor b,13) connected to the temperature controller (not shown). The above the room temperature heat is provided the temperature controller through the leads (b, 4) and the lower temperature obtained from ice in the ice compartment of the thermostat (d, 1).

Odorants

The odorant used in the experiment was a mixture of ethyl butyrate, eugenol, and (+) and (−) carvone in water at a concentration of 1.6 mM. Because the water/air partition coefficient for all odorants we used in our experiments is very low (~10^{-4}), the concentration of the odorants in the head space is in ~ 100 nM range. For example, the concentration of Eugenol in head space can be estimated using Amoore-Buttery equation for the water/air partition coefficient, K_{aw}, from value of vapor pressure, solubility in water and molecular weight ([1]:

K_{aw}= (((55.5/S-0.0555)xM+1)xPx0.97x$10^{—6}$,

where P is vapor pressure in mm Hg, S is solubility in water in g/L of the pure odorant at 25 ^{o}C and M is its molecular weight. for Eugenol we have P=0.0226 mm Hg; S=2.47 g/L; M=164.2 g/mol. According to the Amoore-Buttery equation, K_{aw}=8.08×10^{-5}. This value of K_{aw} for Eugenol agrees well with that obtain experimentally [2]. Thus, the concentration of Eugenol in head space =8.08×10^{-5}×0.016×10^{-3} M=1.3×10^{-7} M=130 nM

Single transduction in the initial events of olfaction

Olfaction in most mammals begins with the act of sniffing [3] which transports odorant molecules into the nose and delivers them to the mucus layer covering the olfactory epithelium. OSNs have hair-like cellular structures protruding apically, called olfactory cilia. These cilia harbor the sensory apparatus, including the OR proteins, heterotrimeric G-proteins, and downstream second messenger components involved in the GPCR cascade. The cilia are where olfactory transduction occurs. [4]. The binding of an odorant molecule to an odorant receptor [5, 6] on a cilium induces a conformational change of the receptor, causing the activation of an interacting G-protein. In turn, the G-protein alpha subunit stimulates the enzymatic activity of an adenylyl cyclase (AC) generating an increase in the cytoplasmic concentration of cyclic AMP (cAMP) [7, 8]. Cyclic nucleotide-gated channels (CNGC) located in the ciliary membrane are directly activated by cAMP, causing a depolarizing influx of Na^{+} and Ca^{2+} -ions [9]. The intracellular increase of Ca^{2+} concentration directly gates Ca-activated Cl channels. The opening of Ca-activated Cl channels causes an efflux of Cl^{-} ions from the cilia, corresponding to an inward current that further contributes to the depolarization of OSNs [10, 11]. Several Ca-dependent feedback mechanisms may contribute to deactivation. The cilia contain a phosphodiesterase that, after being activated by the complex Ca^{+2}-Calmodulin (CaCaM), hydrolyzes cAMP [12]. However, the role of the phosphodiesterase in the fast adaptation is questioned [13]. The complex CaCaM and possibly other Ca-binding proteins decrease the sensitivity of the CNG channel to cAMP [14, 15, 16]. The activation of CaCaM-dependent protein kinase II (CaMK) inhibits AC activity [17]. Finally, the intracellular Ca^{2+} concentration is reduced by Ca-extrusion through a Na+/Ca^{2+} exchanger [18]. The combined ion currents shift the olfactory neuronal membrane potential to the above threshold level when it triggers an action potential in the ORN axon that projects directly to OB and communicates with the synaptic connection of mitral and other cells in the glomerulus [19]. From the olfactory bulb, the information is further sent to the higher brain regions for

recognition of the signal. Finally, the odorant is cleared from mucus, and the process begins again [20].

Example calculations of thermodynamic parameters of EOG processes using Arrhenius-Eyring equations.

The energy of activation E_a can be calculated directly from Eq. (5) using the value of the Arrhenius slope (-1.84±0.18)

E_a=-2.3R(slope×$10^{3)}$=-2.3×1.98(-1.84×$10^{3)}$=8379 cal/mol

E_a=8.4±0.8 kcal/mol

The entropy change, ΔS at 25 ^{o}C, can be obtained from the value of the Arrhenius plot intercept (6.47±0.62) by using Eq. (12).

ΔS=2.3R[logA-log(k_b/h)-log(eT)]=2.3×1.98(6.47-10.32-2.91)=-30.8±2.0 calK^{-1}mol^{-1}

The enthalpy, ΔH, at 25 ^{o}C is calculated by Eq. (10)

$\Delta H=E_a-RT$=8379-590=7789 cal/mol

ΔH=7.8±0.7 kcal/mol

The energy contribution due to the entropy change at 25 ^{o}C is equal to

$T\,\Delta S$=298(-30.78)=-9172 cal/mol

$T\,\Delta S$=-9.2±0.8 kcal/mol

The Gibbs free energy change, ΔG, is calculated by Eq. (8):

$\Delta G= \Delta H- T\,\Delta S$=7789+9172=17962 cal/mol

ΔG=16.9±1.2 kcal/mol

Example calculations of thermodynamic parameters of EOG processes using cumulative frequency distributions of EOG rate constant at two temperatures from the experimental results.

Using Eq. (13) we can calculate the activation energy, E_a

E_a=log(1.8/1.3)×(2.3×293.4×298.4)/5=6078 cal/mol

E_a=6.1±02 kcal/mol

From Eq. (14) we have:

$log\ A_1$=log1.3+6078/2.3×1.98×293.4=4.7

$log\ A_2$=log1.8+6078/2.3×1.98×298.4=4.7

From Eq.(15) we have

ΔS=2.3×1.98(4.7-13.23)=-38.8±3.0 calK^{-1}mol^{-1} (at T=24 ^{o}C)

$T\,\Delta S$=298×(-38.8)=-11562 cal/mol

$T\,\Delta S$=-11.6±0.8 kcal/mol

According to Eq.(16)

ΔH=6078-590=5488 cal/mol

ΔH=5.5±0.4 kcal/mol

From Eq. (8) we have

ΔG=5488+11562=17050 cal/mol

ΔG=17.1±1.1 kcal/mol

References

1. Amoore JE, Buttery RG. Partition-Coefficients and Comparative Olfactometry. Chemical Senses & Flavour. 1978;3(1):57-71. PubMed PMID: ISI:A1978ET62700008.
2. Martins MAR, Silva LP, Ferreira O, et al. Terpenes solubility in water and their environmental distribution. Journal of Molecular Liquids. 2017 2017/09/01/;241(Supplement C):996-1002. doi: https://doi.org/10.1016/j.molliq.2017.06.099.
3. Kepecs A, Uchida N, Mainen ZF. The Sniff as a Unit of Olfactory Processing. Chemical Senses. 2006;31(2):167-179. doi: 10.1093/chemse/bjj016.
4. Dennis JC, Aono S, Vodyanoy VJ, et al. Morphology and functional anatomy of the mammalian nasal cavity. In: Doty RL, editor. Handbook of Olfaction and Gustation. 3d ed: Wiley, John & Sons; 2013.
5. Lancet D, Pace U. The Molecular-Basis of Odor Recognition. Trends Biochem Sci. 1987 Feb;12(2):63-66. PubMed PMID: ISI:A1987G220900010.
6. Buck L, Axel R. A novel multigene family may encode odorant receptors: a molecular basis for odor recognition. Cell. 1991;65(1):175-87.
7. Breer H. Olfactory receptors: molecular basis for recognition and discrimination of odors. Anal Bioanal Chem. 2003 Oct;377(3):427-433. PubMed PMID: ISI:000185485600007.
8. Breer H. Sense of smell: recognition and transduction of olfactory signals. Biochem Soc Trans. 2003 Feb;31:113-116. PubMed PMID: ISI:000181161000024.
9. Zufall F, Firestein S, Shepherd GM. Analysis of Single Cyclic-Nucleotide Gated Channels in Olfactory Receptor-Cells. J Neurosci. 1991 Nov;11(11):3573-3580. PubMed PMID: ISI:A1991GP89800024.
10. Kleene SJ. The Electrochemical Basis of Odor Transduction in Vertebrate Olfactory Cilia. Chem Senses. 2008 August 14, 2008;33:839-859. doi: 10.1093/chemse/bjn048.
11. Pifferi S, Boccaccio A, Menini A. Cyclic nucleotide-gated ion channels in sensory transduction. FEBS Letters. 2006 2006/05/22/;580(12):2853-2859. doi: https://doi.org/10.1016/j.febslet.2006.03.086.
12. Borisy F, Ronnett G, Cunningham A, et al. Calcium/calmodulin-activated phosphodiesterase expressed in olfactory receptor neurons. J Neurosci. 1992 March 1, 1992;12(3):915-923.
13. Boccaccio A, Lagostena L, Hagen V, et al. Fast adaptation in mouse olfactory sensory neurons does not require the activity of phosphodiesterase. J Gen Physiol. 2006 Aug;128(2):171-84. doi: 10.1085/jgp.200609555. PubMed PMID: 16880265; PubMed Central PMCID: PMCPmc2151529. Eng.
14. Balasubramanian S, Lynch JW, Barry PH. Calcium-dependent Modulation of the Agonist Affinity of the Mammalian Olfactory Cyclic Nucleotide-gated Channel by Calmodulin and a Novel Endogenous Factor. The Journal of membrane biology. 1996 1996/07/01;152(1):13-23. doi: 10.1007/s002329900081.
15. Bradley JR, Johannes; Frings, Stephan. Regulation of cyclic nucleotide-gated channels. Current Opinion in Neurobiology. 2005;15(3):343-349.
16. Chen TY, Yau KW. Direct modulation by Ca(2+)-calmodulin of cyclic nucleotide-activated channel of rat olfactory receptor neurons. Nature. 1994 Apr 7;368(6471):545-8. doi: 10.1038/368545a0. PubMed PMID: 7511217; eng.
17. Yang YD, Cho H, Koo JY, et al. TMEM16A confers receptor-activated calcium-dependent chloride conductance. Nature. 2008 Oct 30;455(7217):1210-5. doi: 10.1038/nature07313. PubMed PMID: 18724360; eng.
18. Matthews HR, Reisert J. Calcium, the two-faced messenger of olfactory transduction and adaptation. Current Opinion in Neurobiology. 2003 2003/08/01/;13(4):469-475. doi: https://doi.org/10.1016/S0959-4388(03)00097-7.
19. Harel D, Carmel L, Lancet D. Towards an odor communication system. Computational Biology and Chemistry. 2003 2003/05/01/;27(2):121-133. doi: https://doi.org/10.1016/S1476-9271(02)00092-0.
20. Getchell TV, Margolis FL, Getchell ML. Perireceptor and receptor events in vertebrate olfaction. Prog Neurobiol FIELD Full Journal Title:Progress in neurobiology. 1984;23(4):317-45. PubMed PMID: 85191403.